ON OPTIMAL PROGRAMMED PWM WAVEFORMS FOR DC-DC CONVERTERS

Andrew Wang *Seth R. Sanders*

Department of Electrical Engineering and Computer Science
University of California, Berkeley
Berkeley, CA 94720 U.S.A.

Abstract: *The regular switching action of a Pulse Width Modulated (PWM) circuit generates conducted and radiated electromagnetic interference (EMI), and may also generate acoustical disturbances. Programmed pulsed-width modulation techniques have been applied using various methods to control harmonics inherent in switched power circuits. In this paper, a method to generate an optimal programmed switching waveform for a DC-DC converter is presented. Also, a practical implementation of a circuit to generate such a waveform is given.*

1. INTRODUCTION

This paper investigates methods for reducing unwanted spectral components of circuit waveforms in PWM power conversion circuits. Fig. 1 shows a portion of a 50% duty cycle square wave and its spectral components. In many applications, the concentration of power at discrete frequencies is undesirable. For instance, it may be necessary to reduce an annoying audible tone, or an electromagnetic interference (EMI) specification may be satisfied by reducing peak harmonic components, or one might be able to reduce the size and weight of filter elements by reducing peak spectral components.

The main approaches considered in this paper rely on the fact that it is possible to operate a PWM type power circuit with a time-varying switching frequency provided the average duty cycle is not disturbed. In particular, we demonstrate how the switching instants can be perturbed in programmed ways so that the spectral energy of a given circuit waveform is effectively spread out. Section 2 of the paper reviews the main techniques considered in the literature. Sections 3 and 4 illustrate the application of these methods in the context of a DC-DC converter. Experimental results are presented in Section 5, and a discussion of the implementation is given in Section 6.

. 2. REVIEW OF EXISTING TECHNIQUES FOR HARMONIC CONTROL

The first method of harmonic control to be discussed can be termed programmed pulse-width modulation. In programmed PWM, a precomputed set of turn-on and turn-off times (or angles) is stored in a memory or look-up table, and then accessed periodically by a control circuit. This method can be used to generate

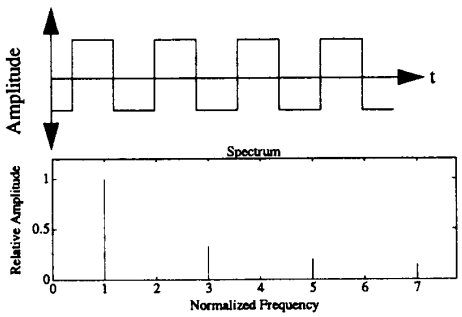

Fig. 1 Square wave and associated spectrum

steady state waveforms and therefore has found applications in inverters and DC-DC converters. Some of the earliest work in harmonic control is due to Turnbull [1]. In the context of an inverter, Turnbull calculated the necessary turn-on and turn-off angles to generate a modified square-wave that had no third or fifth harmonic components. Waveform symmetry properties, namely quarter-cycle even symmetry and half-cycle odd symmetry, were maintained to assure that no even harmonics were generated. Reference [1] also noted that certain three-phase connections blocked triple-n (i.e. third, sixth, etc.) harmonic components, and that it was advantageous in these three-phase connections to select the switching angles to null the fifth and seventh harmonics. The later work of Patel and Hoft [2,3] generalized the results of Turnbull by allowing, in principle, an arbitrary number of turn-on and turn-off transitions per cycle. The waveforms in [2,3] contained the necessary quarter- and half-cycle symmetries to avoid the introduction of even harmonics. Reference [2] applied a Newton-type numerical algorithm to determine the switching angles that resulted in a prescribed set of harmonics being nulled. Reference [3]extended the method of [2] to specify the amplitude of the fundamental as well as nulling a given set of harmonic components. The paper [5] of Goodarzi and Hoft took a similar approach to the harmonic control problem, but minimized a weighted square sum of certain harmonic components with the constraint that the amplitude of the fundamental assumed a constant value. This method also relied on a Newton-type numerical scheme for determining the optimal switching angles. A summary of the programmed PWM methods is given in the paper [4] of Enjeti et al.

0-7803-0695-3/92 $3.00

A second approach to harmonic control involves randomized switching, and has been quite successfully applied by a number of researchers. It is of interest that with the randomized type switching, one is not restricted to a set of precomputed waveforms. An example of this is the recent work of Tanaka et al. [6]. The focus in [6] was not on the lower harmonics of the fundamental switching frequency, but on much higher frequency noise generated by the turn-on and turn-off process in a given DC-DC converter. This work relied on the spectral characterization of the noise generated by each type of transition (turn-on or turn-off), as studied in the authors' earlier papers [7,8]. Using characterizations of the relevant transitions as impulse responses, the authors were able to deduce the form of the spectrum of a periodic sequence of turn-on and turn-off transitions. Reference [6] then added a random timing component to the switching sequence in an attempt to spread high frequency harmonic components. The random timing component introduced in [6] evidently corresponds to a frequency (or phase) modulation with white noise. The experimental results reported in [6] state that high frequency spectral components are reduced in magnitude by a factor of approximately two or three via the spectral spreading.

A very effective use of randomized switching has been reported in [9]. Reference [9] used a scheme very similar to that of [6] to reduce acoustical and electrical noise harmonics in a PWM induction motor drive. The main difference in [9] with respect to [6] is the use of band-limited modulation. In particular, reference [9] relied on Carson's rule for the estimation of spectral bandwidths in wideband frequency modulation. The result was an effective shaping of the spectrum to reduce harmonic peaks. A reduction of the peak spectral components by a factor of approximately five was obtained. The paper [9] noted that the randomized switching could be implemented by generating the switch times in an on-line manner using a random number generator and shaping filter or by storing a long sequence (a few seconds in length) of switching periods.

Another implementation of randomized switching is in the paper of Legowski et al. [10] where a random PWM technique is used to generate a high-quality sine wave inverter output. One apparent drawback of the scheme of [10] is the necessity of increasing the average switching frequency by a large factor.

In [14], formulas are presented for estimating the power spectra of several randomized switching schemes. The formulas are verified using Monte-Carlo simulations.

3. PROGRAMMED SWITCHING SEQUENCES FOR DC-DC CONVERTERS

As an example of a circuit where the use of programmed PWM can be compared with regular PWM, we consider the forward converter of Fig. 2. To design a programmed switching sequence for this converter, it is first necessary to choose a waveform that we wish to optimize using the programmed PWM. Possible criteria on the optimization can be based on the FCC regulations on conducted EMI and radiated EMI, for instance. Our approach for meeting the FCC regulations is to spread out the spectral energy of the EMI to reduce the overall peak amplitude. We accomplish this by first defining a desired spectral envelope for the selected waveform. Then, we use a constrained min-max optimization on the switching instants to make the spectrum of the waveform fit under this envelope.

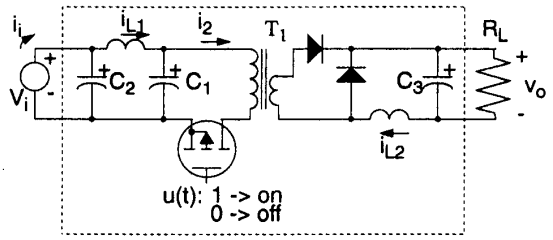

Fig. 2 Forward converter power path

Circuit Waveforms

For steady state operation, most of the voltage and current waveforms occurring in the converter can be approximated as filtered versions of the PWM waveform which drives the switch. Some of the waveforms may also contain significant switching transients, which we also consider.

The programmed PWM waveform is similar to the regular PWM waveform except that the turn-on and turn-off times are varied. Two possible parameterizations for the programmed PWM are given in Fig. 3. In each case, the period is increased by an integer K so that it contains K subperiods. Subperiod k has length T_k and duty cycle D_k. For the "triangle" parameterization shown in Fig. 3, we require that the "on" time of length T_kD_k within each subperiod k must be centered within the subperiod. Although this restricts the range of admissable PWM waveforms, it is easier to implement in practice using a programmable triangle wave, as will be explained in Section 6. The "sawtooth" parameterization can be used to generate arbitrary PWM waveforms, but requires a programmable sawtooth wave. We have found from optimizations with both parameterizations that the differences in numerical results are not very significant. Therefore, we will limit our discussion below to the triangle parameterization waveform, noting that results obtained with the sawtooth parameterization are similar.

Optimization Criteria

The design goal in our experimental work is the suppression of conducted EMI. Conducted EMI onto distribution lines is detrimental and therefore regulated by various agencies such as the FCC and VDE. The noise is generally measured with the use of a Line Impedance Stabilization Network (LISN) which presents a specified impedance to the device under test and has a voltage output for noise level measurement. The FCC specified LISN presents an impedance that is almost constant above 1 MHz and that drops off slightly below 1 Mhz, as given in reference [12]. With this LISN, typical FCC conducted noise limits [13] are shown in Fig. 4. Similar VDE regulations are also shown. A reasonable optimization goal in light of this regulation is to reduce the peak harmonic amplitude, weighted by the applicable curve in Fig. 4.

Another possible goal is the reduction of radiated EMI, which is caused by high frequency components of switching transients.

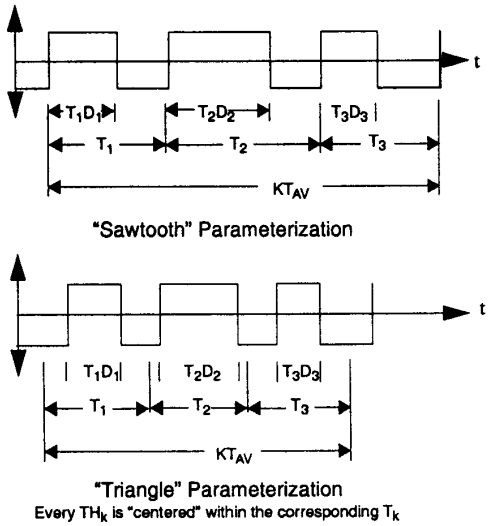

Fig. 3 Possible parameterizations of PWM waveform

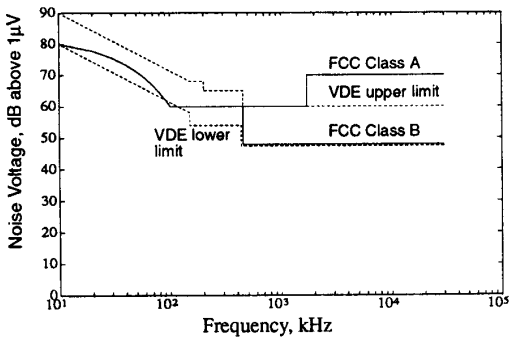

Fig. 4 FCC and VDE conducted EMI limits

After implementing appropriate physical layout by elimination of large area current loops, and the use of shielding, a programmed PWM waveform can help spread the spectrum to reduce peak harmonics in the electromagnetic radiation. We could attempt to make the reshaped radiation spectrum fit under the curve of the FCC limits on electromagnetic radiation, shown in Fig. 5.

Programmed Waveform Constraints

For our purposes, the programmed PWM waveform must meet several constraints, both in the time and frequency domains.

C1) The programmed PWM waveform must have the same average period and the same average duty cycle as the original PWM waveform.

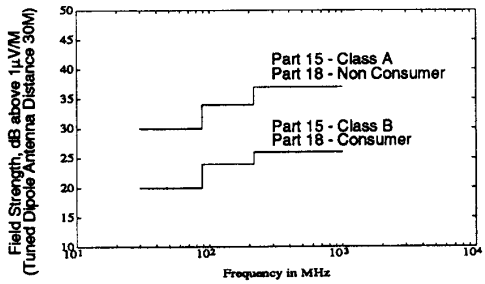

Fig. 5 FCC radiation limits, U.S. code Parts 15 and 18, Title 47

C2) Every pulse must be longer than some minimal width, due to semiconductor switch constraints.

C3) For control purposes, the average duty cycle of the new waveform must be continuously variable via a control signal.

C4) The lowest frequency harmonic in the programmed PWM waveform must be well above the bandwidth f_p of the control loop. Otherwise, the control loop will modify the programmed PWM waveform, even in the steady-state.

Constraint (C4) limits the maximum number of subintervals in the programmed waveform before it repeats. Let f_o be the original switching frequency, and K be the (integral) number of subintervals in the programmed waveform. Then, K must be less than (f_o/f_p).

4. GENERATION OF A PROGRAMMED SWITCHING WAVEFORM

In the previous section, we discussed the parameterization of the programmed PWM waveform, and the frequency and time domain constraints on it. Also, we described possible optimization goals for the waveform. In this section, we formulate equations necessary for the optimization procedure.

We call the waveform that we are trying to optimize (such as the current drawn from the source) the "output waveform" of our optimization. It is the sum of an "ideal" waveform and a "transient" waveform as shown in Fig. 6. The ideal portion of the output waveform is generated by assuming there are no parasitics and that the switching components are ideal. The transient waveform contains only the turn-on and turn-off transient components, which are due to circuit parasitics.

The Fourier series coefficients of the output waveform are denoted $\phi[n]$. In the optimization, we first generate an equation for the relationship between the programmed waveform parameters $(T_1, T_2, \ldots, T_{K-1}, D_1, D_2, \ldots, D_{K-1})$ and $\phi[n]$. Next, we weight $\phi[n]$ with a simple function to specify an optimization target for the relative harmonic amplitudes. Finally, a few constraints are specified, and then the optimization performed.

We denote the period of the original PWM waveform by T_{AV}, which must also be the average length of the subperiods in the pro-

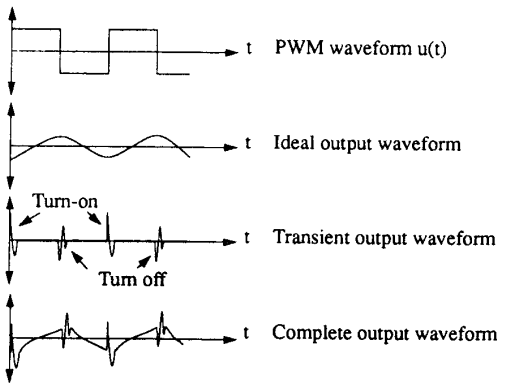

Fig. 6 Output waveform composition

grammed PWM, due to constraint (C1). Similarly, again by (C1), the average duty cycle D_o of the programmed PWM must be the same as that of the regular PWM. In the additional definitions below, functions of time are noted in lower case. Their Fourier series representations are also in lower case, as bracketed functions of n. Fourier transforms are in upper case.

- $s_{ON}(t)$: Function containing a unit impulse at each turn-on instant
- $s_{OFF}(t)$: Function containing a unit impulse at each turn-off instant
- u(t): PWM switching waveform
- $H_{ON}(\omega)$: Fourier transform of turn-on transient
- $H_{OFF}(\omega)$: Fourier transform of turn-off transient
- $\zeta(t)$: Signum function
- $H_1(\omega)$: Transfer function from PWM switching waveform to output waveform
- $\phi_{ID}[n]$: Fourier series coefficients of ideal output waveform
- $\phi_{TR}[n]$: Fourier series coefficients of turn-on and turn-off transient portion of output waveform.
- $\phi[n]$: Fourier series coefficients of complete output waveform.

The period of the programmed PWM waveform is KT_{AV}, therefore, the lowest programmed PWM harmonic occurs at $\omega_o = (2\pi)/(KT_{AV})$. Due to (C1), the last subperiod and its duty cycle are given by:

$$T_K = KT_{AV} - \sum_{k=1}^{K-1} T_k \tag{1}$$

$$D_K = \frac{KT_{AV}D_o - \sum_{k=1}^{K-1} T_k D_k}{T_k} \tag{2}$$

The functions $s_{ON}(t)$ and $s_{OFF}(t)$ are waveforms with impulses at the turn-on times and turn-off times, respectively. Hence, they and their corresponding Fourier series representations $s_{ON}[n]$ and $s_{OFF}[n]$ are functions of $T_1,T_2,...,T_K$ and $D_1,D_2,...,D_K$:

$$s_{ON}(t) = \sum_{m=-\infty}^{\infty}\sum_{k=1}^{K} \delta\left(t - \left(T_1 + T_2 + \ldots + \frac{T_k}{2} - \frac{D_k}{2} - mKT_{AV}\right)\right) \tag{3}$$

$$s_{OFF}(t) = \sum_{m=-\infty}^{\infty}\sum_{k=1}^{K} \delta\left(t - \left(T_1 + T_2 + \ldots + \frac{T_k}{2} + \frac{D_k}{2} - mKT_{AV}\right)\right) \tag{4}$$

$$s_{ON}[n] = \sum_{k=1}^{K} e^{(-jnw_o)\left(T_1+T_2+\ldots+\frac{T_k}{2}-\frac{D_k}{2}\right)} \tag{5}$$

$$s_{OFF}[n] = \sum_{k=1}^{K} e^{(-jnw_o)\left(T_1+T_2+\ldots+\frac{T_k}{2}+\frac{D_k}{2}\right)} \tag{6}$$

The Fourier series coefficients $\phi_{TR}[n]$ for a waveform that consists only of the turn-on and turn-off noise spikes of the output waveform are easily calculated as shown in Fig. 7. We use the Fourier transforms of the switching transients:

$$\phi_{ON}[n] = s_{ON}[n] \cdot H_{ON}(n\omega_o) \tag{7}$$

$$\phi_{OFF}[n] = s_{OFF}[n] \cdot H_{OFF}(n\omega_o) \tag{8}$$

$$\phi_{TR}[n] = \phi_{ON}[n] + \phi_{OFF}[n] \tag{9}$$

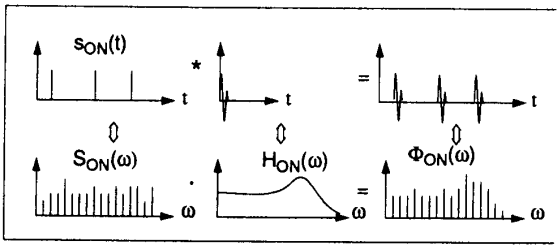

Fig. 7 Turn-on noise waveforms and spectra

To calculate the Fourier series coefficients $\phi_{ID}[n]$ of the "ideal" portion of the output waveform (without turn-on and turn-off noise), we first generate the waveform u(t) driving the switching element. The ideal output waveform is related to the ideal switch waveform u(t) through a linear, time-invariant (LTI) system, which we characterize by the transfer function $H_1(s)$. The calculation of $\phi_{ID}[n]$ is illustrated in Fig. 8, and equations are given below:

$$u(t) = (s_{ON}(t) - s_{OFF}(t)) \quad * \quad \zeta(t) \tag{10}$$

$$\phi_{ID}[n] = (s_{ON}[n] - s_{OFF}[n]) \cdot \zeta(nw_o) \cdot H_1(nw_o) \qquad (11)$$
$$n \in \{1, 2, \ldots \infty\}$$

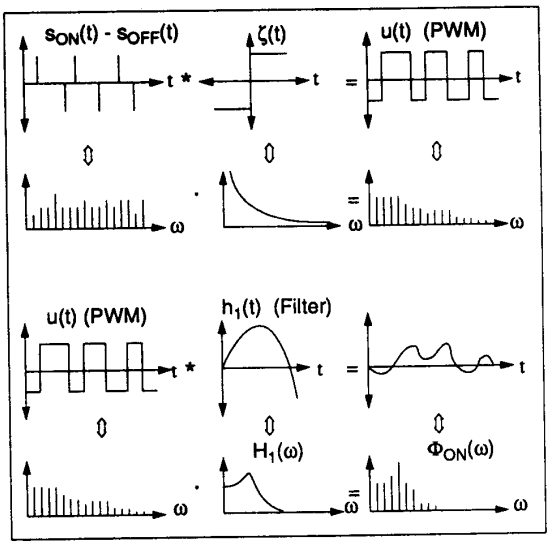

Fig. 8 Ideal portion of output waveform, and associated spectrum

The Fourier series coefficients of the complete output waveform are obtained in (12), by summing the coefficients of the ideal waveform and the transient waveform. An equivalent form is (13), as required for our optimization algorithm.

$$\phi[n] = \phi_{ID}[n] + \phi_{TR}[n] \qquad (12)$$

$$\phi[n] = f_n(T_1, T_2, \ldots, T_{K-1}, D_1, D_2, \ldots, D_{K-1}) \qquad (13)$$

To allow for a target spectral envelope that is not flat, we define a weighting function $\psi[n]$, $n \in \{1, 2, \ldots \infty\}$, where $\psi[n]$ represents the desired relative amplitude of harmonic n. Then the cost function that we attempt to minimize is (14). Thus, the optimization will attempt to make the amplitudes of the harmonics fit under an "envelope" in the shape described by $\psi[n]$.

$$J = \max_n \left(\frac{abs(\phi[n])}{\psi[n]}\right) \qquad n \in \{1, 2, \ldots \infty\} \qquad (14)$$

There are some constraints on the domain of the optimization. From (C3), we have the constraints (15), and from (C2), we obtain (16):

$$\begin{matrix} D_k > D_{min} \\ D_k < D_{max} \end{matrix} \qquad k \in \{1, 2, \ldots, K\} \qquad (15)$$

$$T_k D_k > T_{min} \qquad k \in \{1, 2, \ldots, K\} \qquad (16)$$

Optimization Method

A suitable algorithm for solving the above constrained min-max problem is found in [11]. The algorithm requires that the Fourier series coefficients and the constraint functions be continuous functions of the T_k's and D_k's, and that we have the partial derivatives of these functions. These requirements are satisfied with our formulation. Note that we need to limit the number of Fourier coefficients used in the computation of J in equation to make the computation tractable. It has been found that for conducted EMI calculations, where the lowest frequency harmonics were the largest, using $n \in \{1, 2, \ldots, 1.25K\}$ allowed the minimization algorithm to converge in a reasonable amount of time for a variety of parameters. All of the results were verified when we substituted the resulting optimized T_k and D_k in (14), and found that the calculated value of J was still valid for large values of n.

Although the min-max algorithm was only local, we were able to use it to find useful PWM waveforms. Some optimization weightings gave better results than others in terms of minimizing J, depending on the shape of the weighting. Results are reported below.

5. RESULTS

For an experimental verification, we used an AT&T model 950A DC-DC forward converter, which is designed for a 48VDC input and 5VDC output. With a 2.5Ω load, the PWM waveform was a rectangular wave with a 39% duty cycle. To test the programmed PWM, we replaced the gate drive signal in the forward converter with an EPROM based programmable waveform. The waveform generator was clocked at 16 MHz, and the programmed PWM transitions occurred only on rising clock edges. In this experiment our interest was in steady-state measurements, and hence the circuit was run open-loop.

The optimization target was chosen to be the reduction of the amplitude of the largest harmonic in the current waveform drawn by the converter. The essential configuration of the commercial converter's power path, for study of the lower frequency harmonics, is shown in Fig. 2. The relationship between the switching waveform $u(t)$ and the input current $i_1(t)$ in this circuit topology is nonlinear. However, in order to generate the programmed PWM waveform using the process in Section 4, we make the approximation that i_{L2} is constant within each phase of the switch cycle. Then we have:

$$\frac{I_1(s)}{U(s)} = \frac{I_o}{1 + j\omega R_{L1} C_1 - \omega^2 L_1 C_1} \qquad (17)$$

where R_{L1} is the AC parasitic series resistance in L_1 and I_o is a scaling constant. With $L_1 = 6.2uH$, $C_1 = 3.0uF$, and $R_{L1} = 0.1\Omega$ (which is extrapolated from an LC bridge measurement), this transfer function (17) is shown in Fig. 9. The input waveform was very "clean" in the sense that it did not have appreciable switching transients, so we omitted that portion of the model.

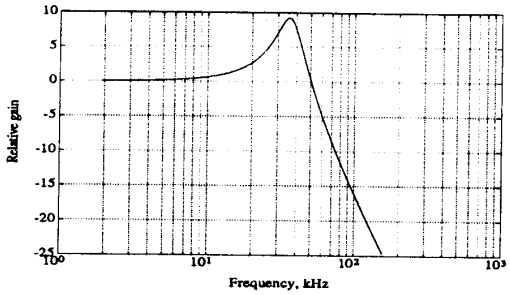

Fig. 9 Transfer function (magnitude), from PWM signal to input current.

The next step was to select a weighting for the desired spectral shape of the input current waveform. We chose the weighting to spread the original first harmonic in the regular PWM to nearby "new" harmonic frequencies in the programmed PWM. Also, the weighting tried to minimize the low frequency harmonics in the programmed PWM. The selected weighting envelope is shown as the dotted line in Fig. 10. The constraints on the D_k's were chosen to be D_{min}=0.3 and D_{max}=0.5, approximately symmetrical around the nominal 39% duty cycle. T_{min} was set to $0.1T_{AV}$, and K to 32 subperiods. The results of the optimization are also shown in Fig. 10 as vertical bars.

Several different spectral weightings were chosen and tested. Attempts at greater suppression of low frequency harmonics caused most of the optimization "effort" to be focused there, and not on making the higher frequency harmonics fit the envelope. It was found that relaxing the requirements on the lower harmonics made the upper harmonics fit the target envelope much more closely. The envelope in Fig. 10 gave a good compromise between reduction in size of the largest harmonic and the peak-to-peak amplitude of the ripple, which is larger with programmed PWM than with regular PWM. For the optimization in Fig. 9, the peak harmonic amplitude is reduced to 34% of the peak harmonic amplitude of regular PWM, resulting in a power reduction in the largest harmonic to approximately one-ninth.

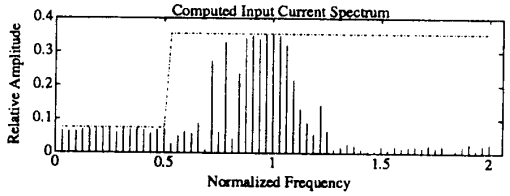

Fig. 10 Target envelope (dashed line) and optimization result (vertical lines)

Measurements with the commercial converter began with a regular 39% duty cycle PWM waveform driving the switch at the original switching frequency, f_o = 125 kHz. The spectrum of the resulting input current waveform (as measured by an HP 4195A network/spectrum analyzer) is shown in Fig. 11. With the programmed PWM waveform computed previously, the measured spectrum of the input current around the original first harmonic is that shown in Fig. 12. The important largest harmonics are very close to those predicted in Fig. 10. Although the lower harmonics are not as well predicted, the power in them is kept very low. The measured peak harmonic amplitude has been reduced from 7.6 mA to 2.7 mA, or 35% of the original level.

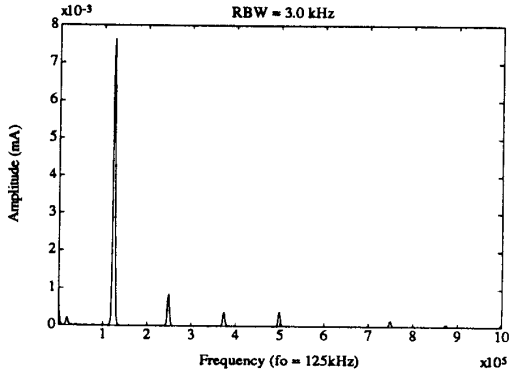

Fig. 11 Measured spectrum of input current, with regular PWM drive (.001Hz - 1MHz)

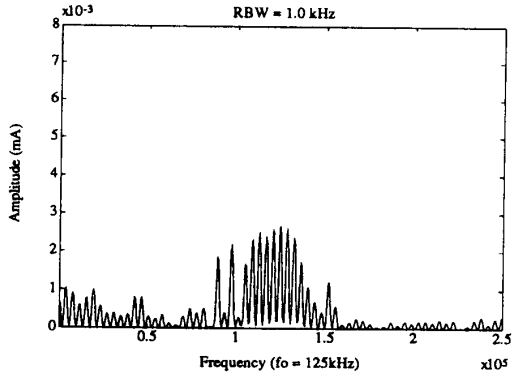

Fig. 12 Measured spectrum of input current, with programmed PWM (.001Hz - 250kHz)

Although no optimization was performed on the higher frequency harmonics, it is noted that their amplitudes are also reduced by varying degrees and could fit under a smaller envelope. For instance, the amplitude of the second harmonic for regular PWM was 0.85 mA. With programmed PWM, the largest harmonic above 180kHz is still at 250kHz, but its amplitude is reduced by 59% to 0.35 mA. Measurements are shown in Fig. 13.

The cost of reducing the size of the peak harmonic includes an increase by 17% of the total power in the harmonics from 1kHz to 1mHz. Also, peak-to-peak input current ripple increased from 28 mA to 38 mA. In addition, low frequency harmonics are now present, but must be kept above the control circuit's bandwidth for the "optimized" PWM to work.

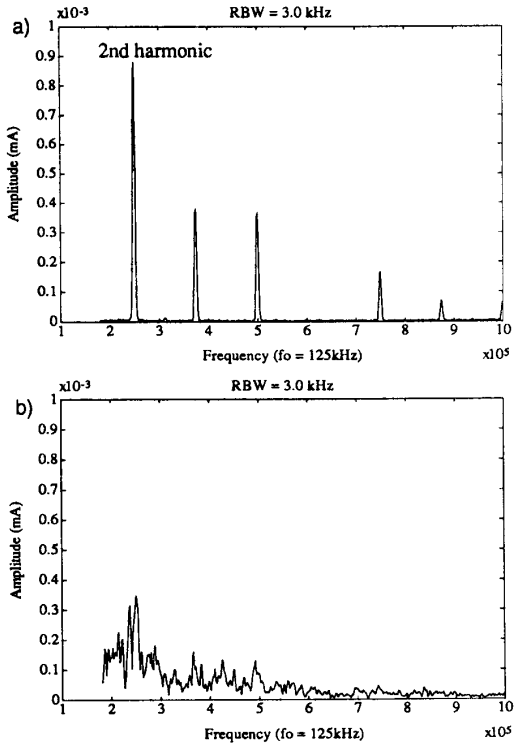

Fig. 13 Measured spectrum of input current, 180kHz - 1MHz:

a) regular PWM
b) programmed PWM

A similar harmonic reduction effect is achieved in [6], where it was found that a 15% random deviation in the switching frequency could approximately halve the peak level in the switching noise amplitude spectrum (as measured by a spectrum analyzer).

6. IMPLEMENTATION

The experimental circuit of Section 5 was run for open-loop testing only, with the PWM waveform generator shown in Fig. 14. It lacks an analog section and therefore the duty cycle control input required for feedback control. For a 32 subperiod sequence, 64 bytes of EPROM are required.

A full implementation of the programmed waveform generator with a continuous control input can be based on a programmable triangle waveform generator. Two numbers are stored for every subperiod. One controls the slope of the triangle waveform, and therefore, the length of the subperiod. The other is added to the control signal, and therefore changes the duty ratio of a given subperiod from the average. The important waveforms and the resulting programmed PWM wave output are shown in Fig. 15. A block diagram implementation is shown in Fig. 16. Note that the average

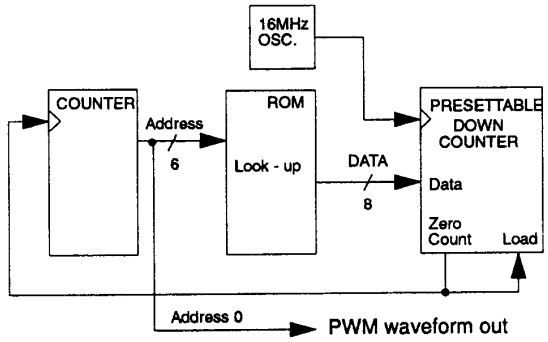

Fig. 14 Simplified PWM generator used in Section 5 for open-loop measurements.

duty cycle can be varied linearly with the standard duty ratio control signal, marked $v_{CONTROL}$ in Fig. 15. However, the linear range is smaller than with regular PWM in this implementation because of the variation in the D_k's. For the experimental result in Section 5, the D_k's only varied from 0.38 to 0.41, so this limitation is not necessarily significant.

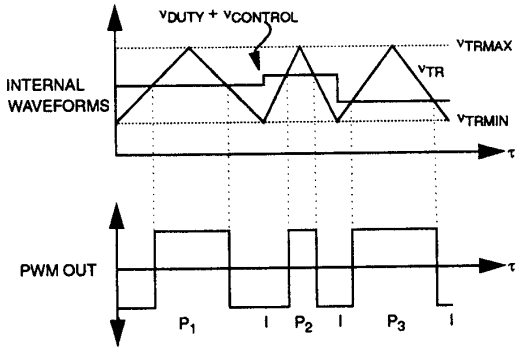

Fig. 15 Programmed PWM generator waveforms

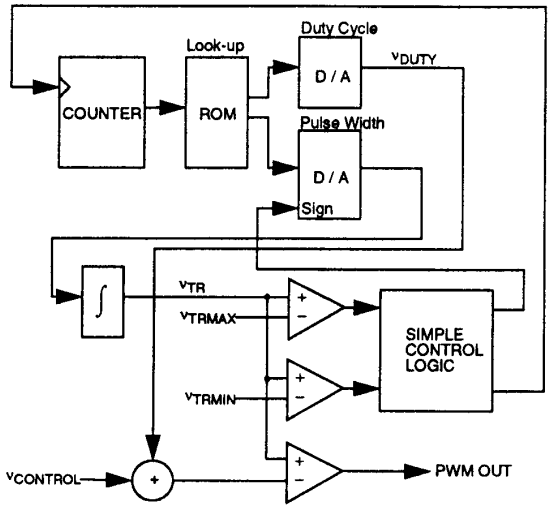

Fig. 16 Programmed PWM generator implementation with control input

7. CONCLUSION

The use of programmed PWM versus regular PWM to reduce the magnitude of the peak harmonic in various DC-DC converter circuit waveforms was investigated. A set of equations for the power supply waveforms was presented, along with an optimization method. We found significant reduction possible with a variety of spectral weightings. In the experimental set-up, a reduction in the power of the peak harmonic to approximately one-ninth was achieved in a commercially available power converter.

Additional work is necessary for implementation of the hardware with a control feedback loop. Also, it would be useful to formulate a method to deal with varying steady-state duty ratios via a look-up table or otherwise. These issues tie in to the robustness of the complete circuit in terms of harmonic control. Another consideration is the effect of programmed PWM on power supply performance, such as transient response.

Since several authors have used randomized PWM to spread spectral components, it would be interesting to study a combination of randomized PWM and the computed PWM presented above.

8. REFERENCES

1. F.G. Turnbull, "Selected Harmonic Reduction in Static DC-AC Inverters," *IEEE Trans. Commun. Electr.*, vol. 83, pp. 374-378, July 1964.

2. H.S. Patel and R.G. Hoft, "Generalized Techniques of Harmonic Elimination and Voltage Control in Thyristor Inverters: Part I - Harmonic Elimination," *IEEE Trans. Ind. Appl.*, vol. IA-9, no. 3, pp. 310-317, May/June 1973.

3. H.S. Patel and R.G. Hoft, "Generalized Techniques of Harmonic Elimination and Voltage Control in Thyristor Inverters: Part I - Voltage Control Techniques," *IEEE Trans. Ind. Appl.*, vol. IA-10, no. 5, pp. 666-673, Sept./Oct. 1974.

4. P.N. Enjeti, P.D. Ziogas, and J.F. Lindsay, "Programmed PWM Techniques to Eliminate Harmonics: A Critical Evaluation," *IEEE IAS Conf. Record*, pp. 418-430, 1988.

5. G.A. Goodarzi and R.G. Hoft, "GTO Inverter Optimal PWM Waveforms," *IEEE IAS Conf. Record*, pp. 312-316, 1987.

6. T. Tanaka, T. Ninomiya, and K. Harada, "Random-Switching Control in DC-to-DC Converters," *IEEE PESC Record*, pp. 500-507, 1989.

7. K. Harada and T. Ninomiya, "Noise Generation of a Switching Regulator," *IEEE Trans. Aerospace Electr. Syst.*, vol. AES-14, no. 1, pp. 178-184, Jan. 1978.

8. T. Ninomiya, M. Nakahara, H. Tajima, and K. Harada, "Backward Noise Generation in Forward Converters," *IEEE Trans. Pow. Electr.*, vol. PE-2, no. 3, pp. 208-216, July 1987.

9. T.G. Habetler and D.M. Divan, "Acoustic Noise Reduction in Sinusoidal PWM Drives Using a Randomly Modulated Carrier," *IEEE PESC Record*, pp. 665-671, 1989.

10. S. Legowski and A. Trzynadlowski, "Power-Mosfet, Hypersonic Inverter with High-Quality Output Current," *IEEE APEC*, pp. 3-7, 1990.

11. E. Polak, "On the Mathematical Foundations of Nondifferentiable Optimization in Engineering Design," *SIAM Review*, Vol. 29, pp. 21-89, March 1987.

12. Federal Communications Commission, "FCC Methods of Measurement of Radio Noise Emissions from Computing Devices," *FCC/OST MP-4*, Dec. 1983.

13. N. Mohan, T.M. Undeland, and W.P. Robbins, *Power Electronics*, John Wiley & Sons, 1989, ch. 17, pp. 427-429.

14. A.M. Stankovic, G.C. Verghese, and R.O. Hinds, "Monte-Carlo Verification of Power Spectrum Formulas for Random Modulation Schemes," submitted to *3rd IEEE Workshop on Computers in Power Electronics*, Aug. 1992, Berkeley, CA.